

Supporting Information

Synergistic catalysis of chloroalkanes dehydrochlorination with acetylene hydrochlorination by immobilized ionic liquid-metal co- catalysts: A DFT study

Yangzhen Jin, Yebin Zhou, Pengze Zhang, Qiuyuan Xiang, Kunming Liu, Yi Liu*, Chunshan Lu*,
Xiaonian Li*

Table of Contents

Figure S1. The structures of metal anions and the adsorption models of TCE, HCl and acetylene on these metal anions.

Figure S2. The structures of metal salts and the adsorption models of TCE, HCl and acetylene on these metal anions.

Figure S3. ΔG of dehydrochlorination of TCE and acetylene hydrochlorination without catalysts.

Figure S4 CuCl_2 catalyzed hydrochlorination mechanism pathways at 260 °C: a) ΔG of CuCl_2 catalyzed mechanism; b) structures of adsorption and transition states.

Figure S5. The adsorption of varying amounts of CuCl_2 in TPPC.

Figure S6. Partial structures of $[\text{Cl-CuCl}]^-$ catalyzed dehydrochlorination mechanism pathways.

Figure S7. Partial structures of CuCl catalytic acetylene hydrochlorination pathways.

Figure S8. Partial structures of CuCl catalytic dehydrochlorination pathways.

Figure S9. The structures of varying amounts of CuCl in TPPC.

Figure S10. The structures of two CuCl ionic pairs in varying amounts of TPPC.

Figure S11. Ionic pairs structures and adsorption models.

Figure S12 KCl-CuCl catalyzed hydrochlorination mechanism pathways at 260 °C: a) ΔG of KCl-CuCl catalyzed mechanism; b) structures of adsorption and transition states.

Figure S13. Partial structures of dehydrochlorination (a) and acetylene hydrochlorination (b) pathways.

Figure S14. The structures of varying amounts of KCl in TPPC- CuCl .

Figure S15. 13KCl-CuCl catalyzed mechanism pathways, a) b) the structure of 13KCl-CuCl ; b) 13KCl-CuCl catalyzed dehydrochlorination for VDC; c) ΔG of $[\text{Cl-}13\text{KCl-CuCl}]^-$ catalyzed dehydrochlorination; d) ΔG of 13KCl-CuCl catalyzed acetylene hydrochlorination pathway.

Figure S16. The structures of $[\text{Cl-}13\text{KCl-CuCl}]^-$ catalyzed dehydrochlorination pathway.

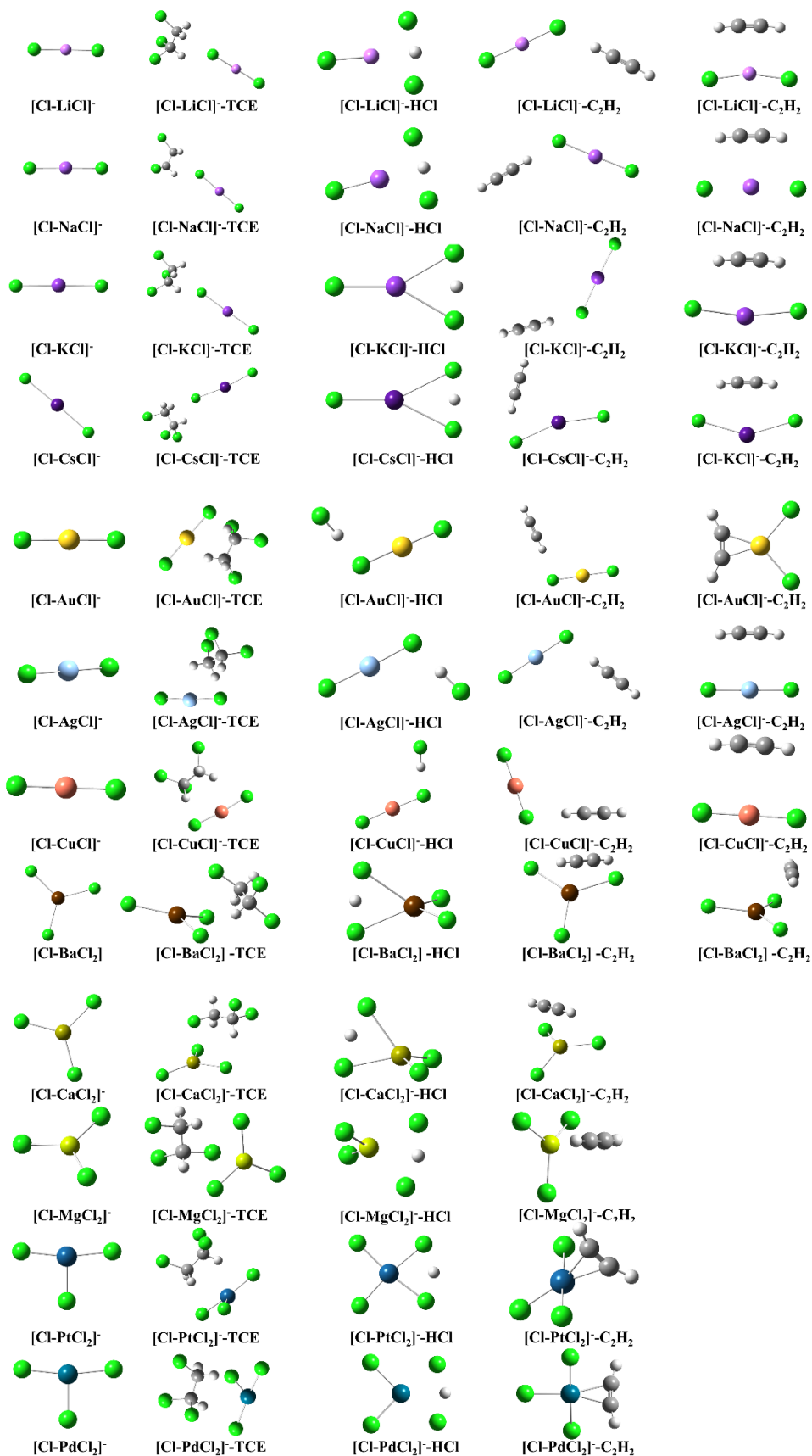
Figure S17. The structures of 13KCl-CuCl catalyzed acetylene hydrochlorination pathway.

Figure S18. Partial structures in generation pathways of copper acetylide.

Figure S19. The adsorption ΔG of olefin products on CuCl , CuCl-CuCl and $[\text{Cl-CuCl}]^-$ at 260 °C.

Figure S20. $[\text{Cl-CuCl}_2\text{-KCl}]^-$ catalyzed dehydrochlorination mechanism pathways at 260 °C.

Table S1. The adsorption $\Delta G_{20\text{ °C}}$ and $\Delta G_{260\text{ °C}}$ of HCl , C_2H_2 and TCE at TPPC- CuCl , TPPC- CuCl_2 and TPPC- KCl-CuCl . (kJ/mol)



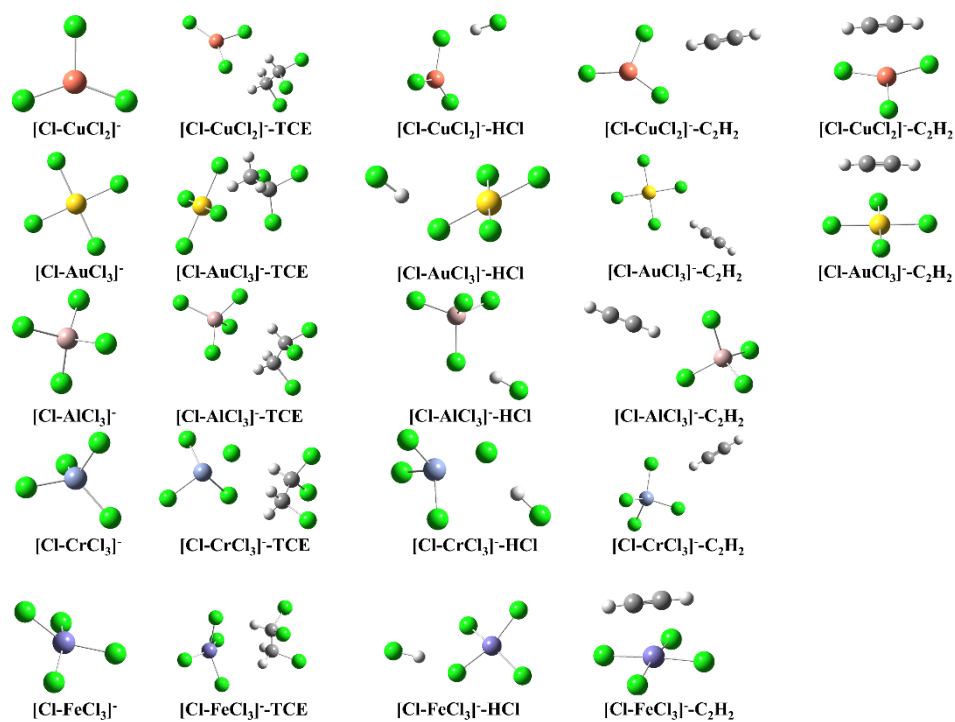
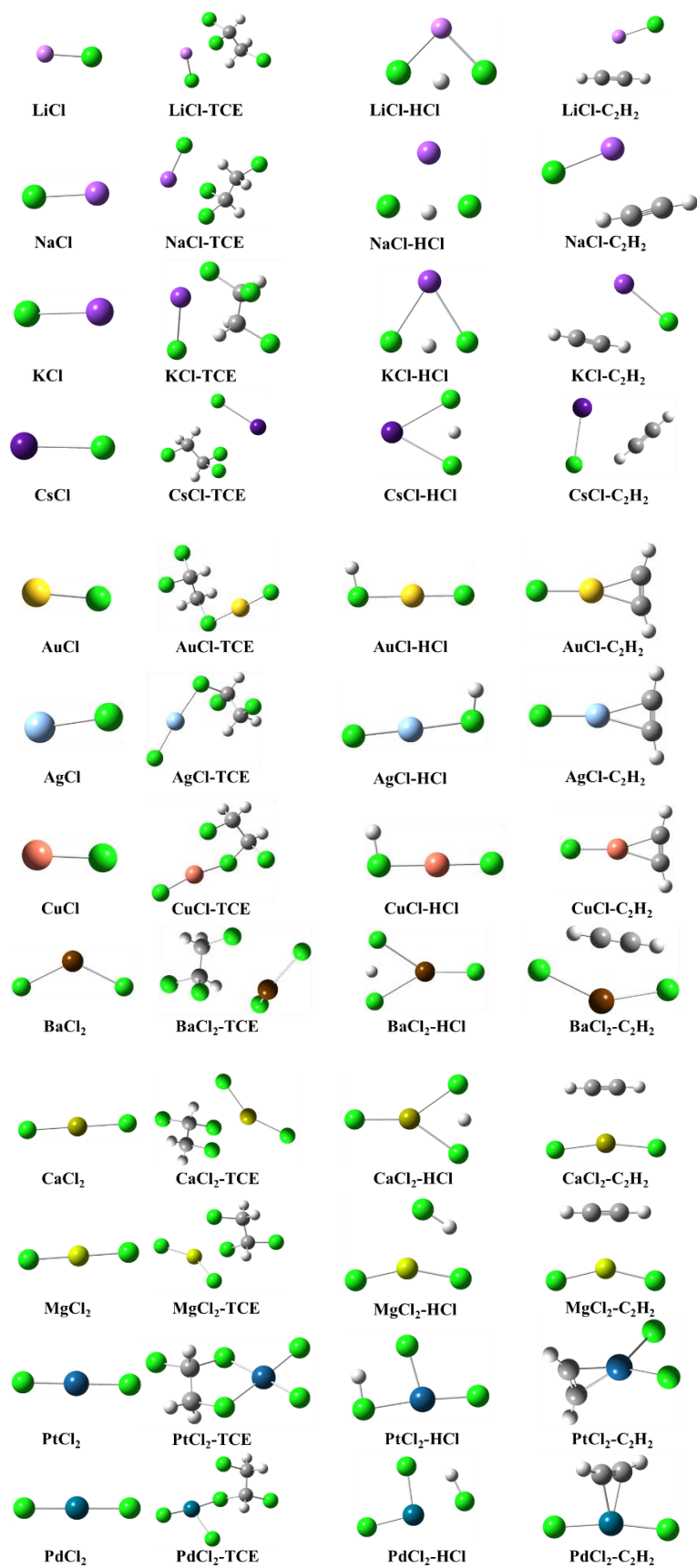


Figure S1. The structures of metal anions and the adsorption models of TCE, HCl and acetylene on these metal anions.



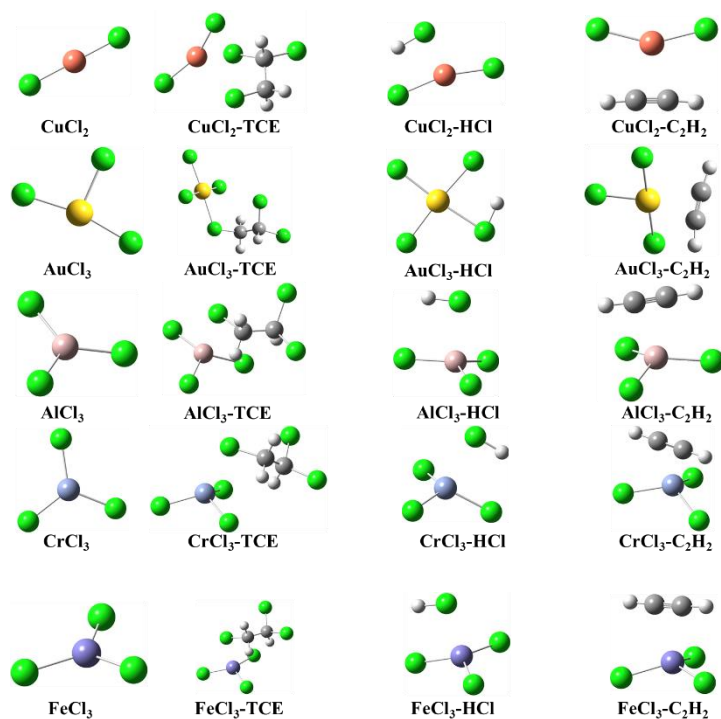


Figure S2. The structures of metal salts and the adsorption models of TCE, HCl and acetylene on these metal anions.

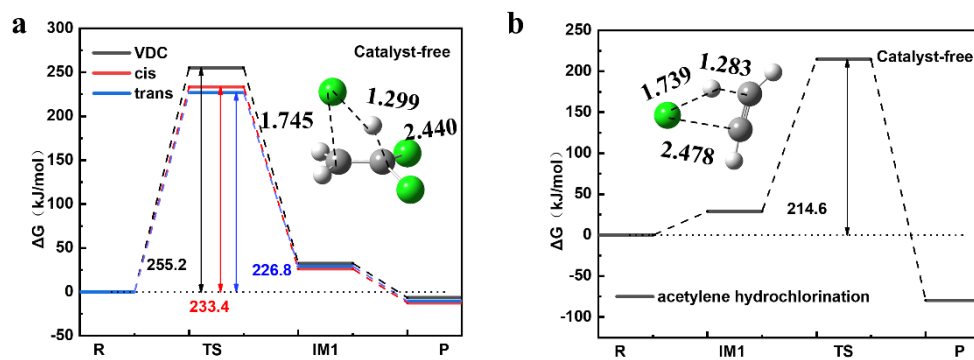


Figure S3. ΔG of dehydrochlorination of TCE and acetylene hydrochlorination without catalysts.

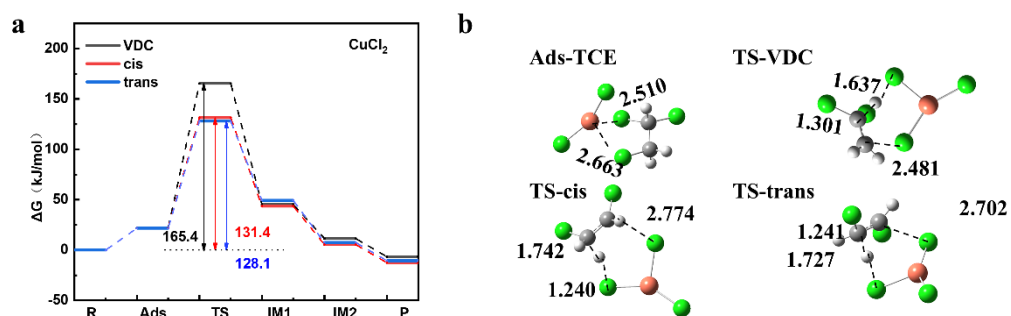


Figure S4 CuCl_2 catalyzed hydrochlorination mechanism pathways at 260 °C: a) ΔG of CuCl_2 catalyzed mechanism; b) structures of adsorption and transition states.

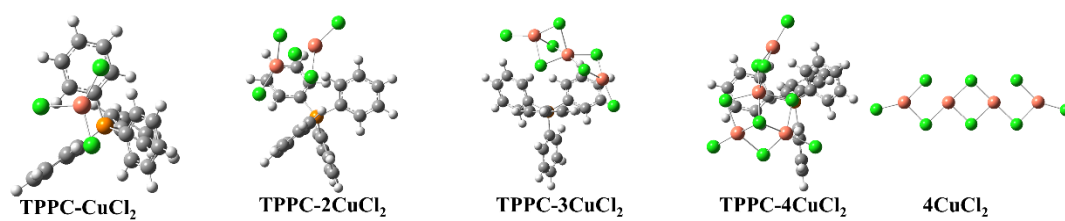


Figure S5. The adsorption of varying amounts of CuCl₂ in TPPC.

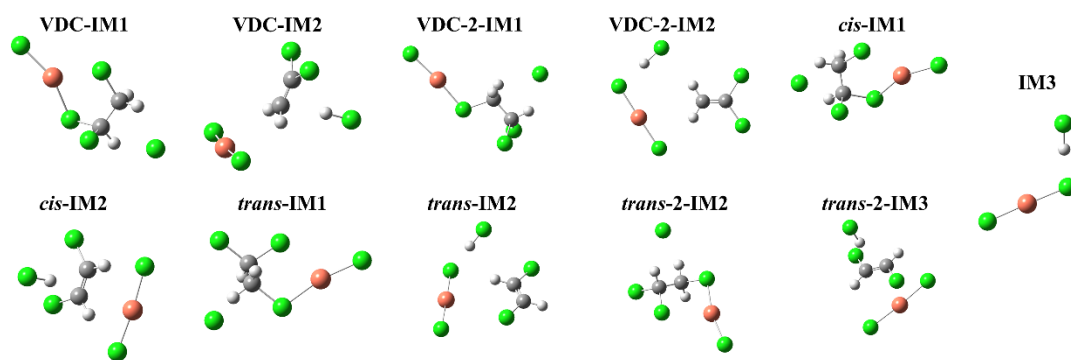


Figure S6. Partial structures of $[\text{Cl-CuCl}]^-$ catalyzed dehydrochlorination mechanism pathways.

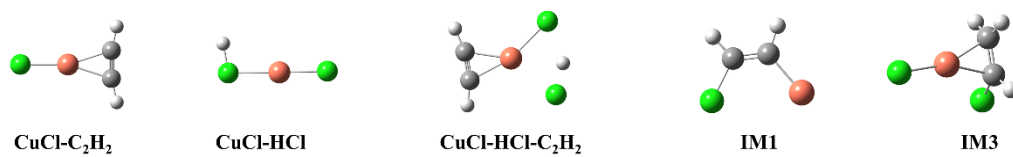


Figure S7. Partial structures of CuCl catalytic acetylene hydrochlorination pathways.

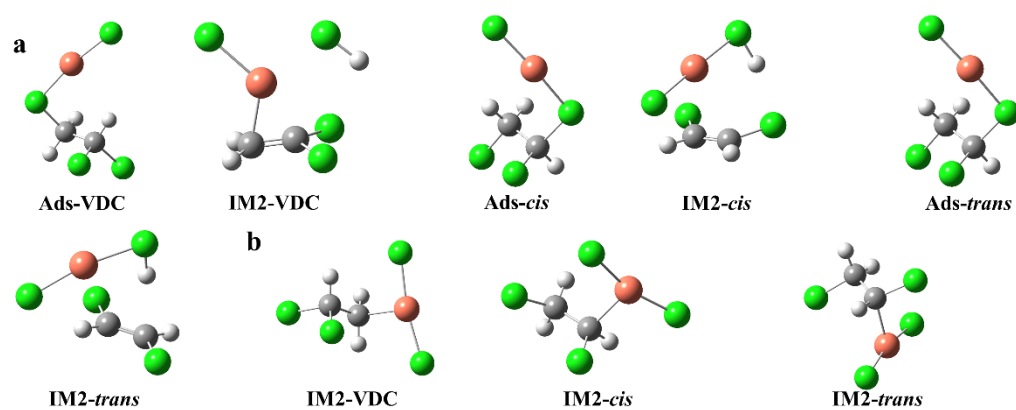


Figure S8. Partial structures of CuCl catalytic dehydrochlorination pathways.

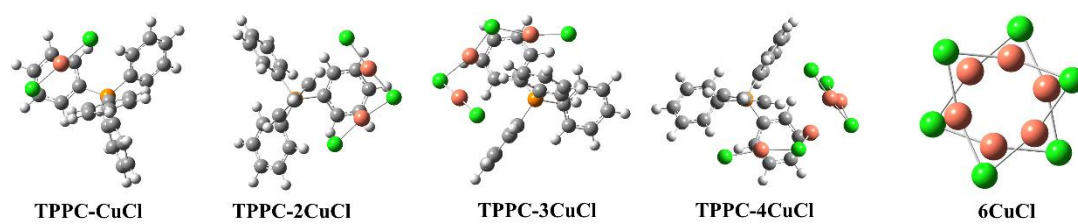


Figure S9. The structures of varying amounts of CuCl in TPPC.

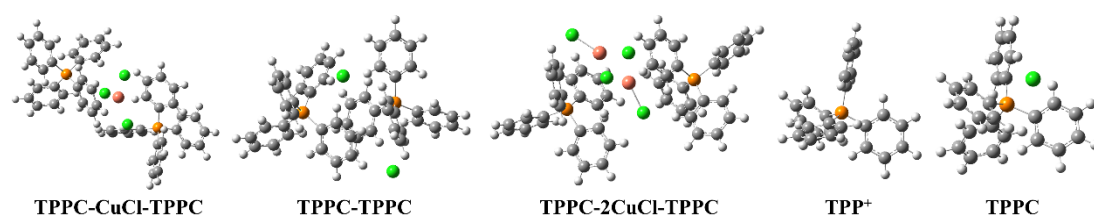


Figure S10. The structures of two CuCl ionic pairs in varying amounts of TPPC.

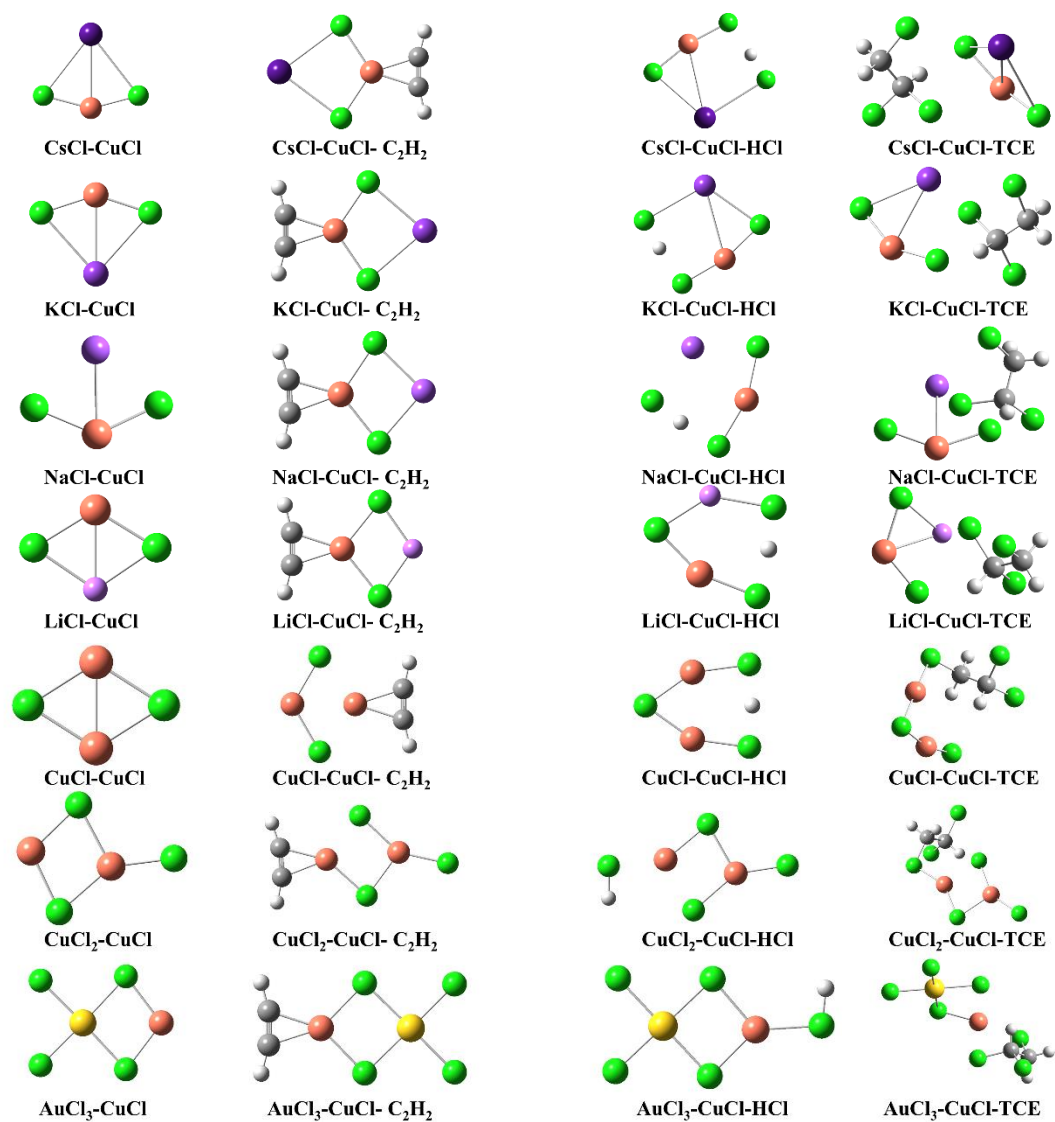


Figure S11. Ionic pairs structures and adsorption models.

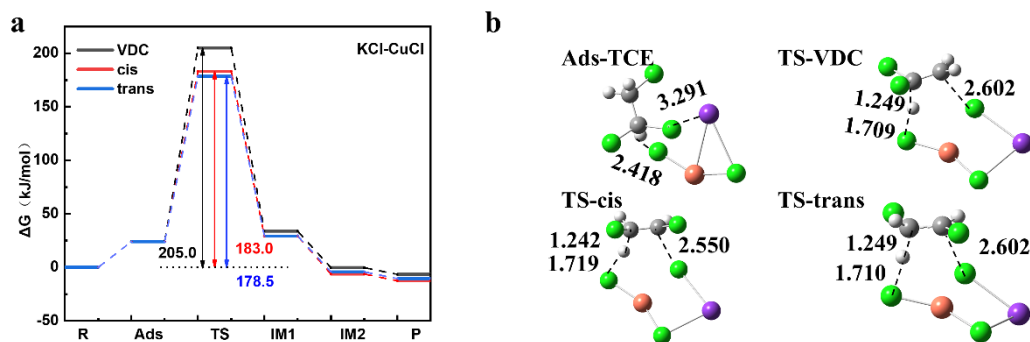


Figure S12 KCl-CuCl catalyzed hydrochlorination mechanism pathways at 260 °C: a) ΔG of KCl-CuCl catalyzed mechanism; b) structures of adsorption and transition states.

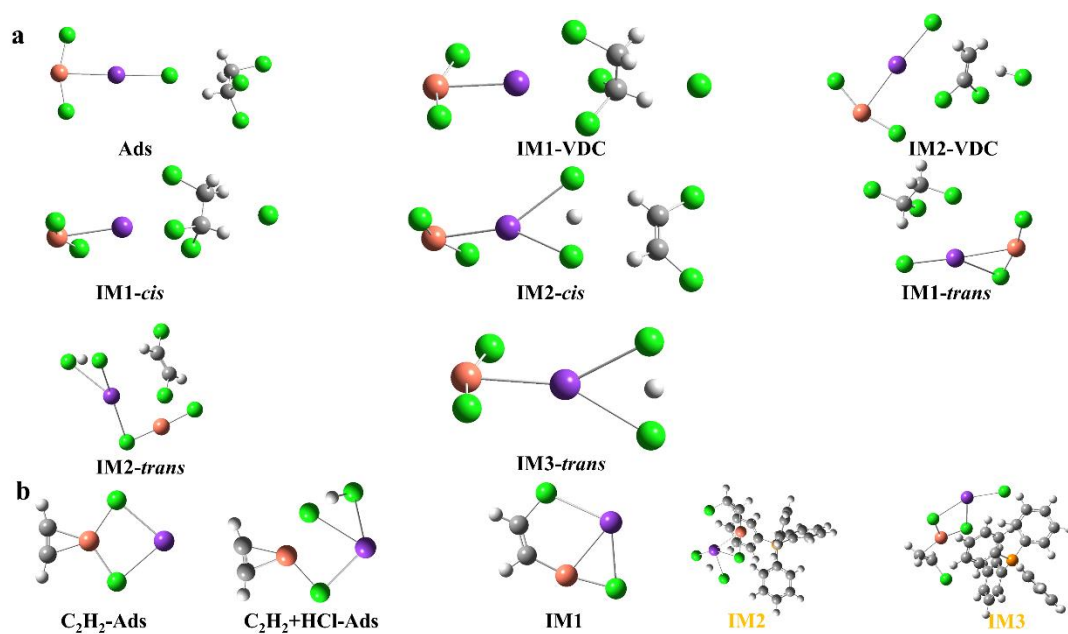


Figure S13. Partial structures of dehydrochlorination (a) and acetylene hydrochlorination (b) pathways.

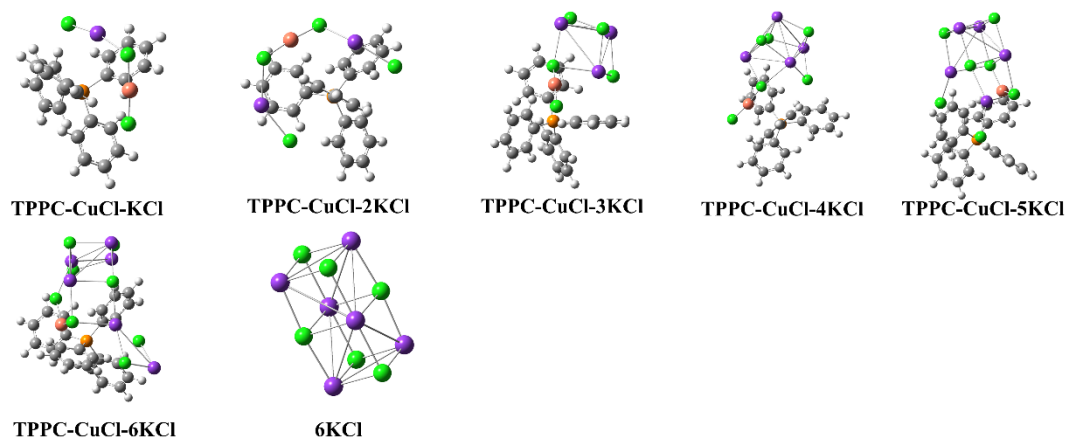


Figure S14. The structures of varying amounts of KCl in TPPC-CuCl.

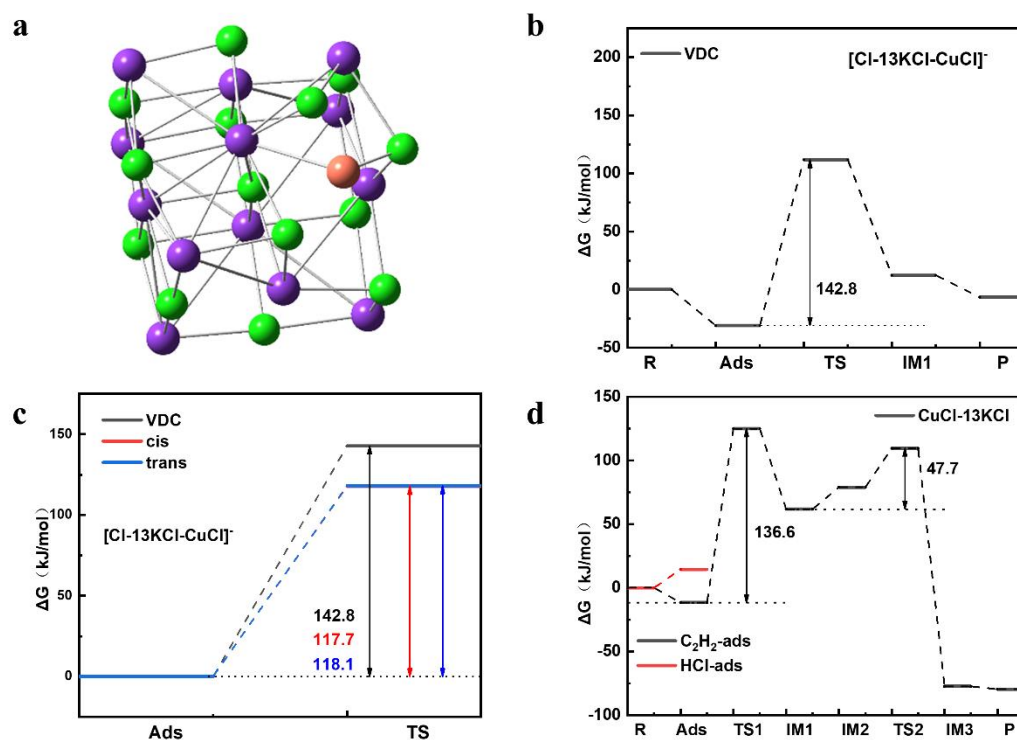


Figure S15. 13KCl-CuCl catalyzed mechanism pathways, a) b) the structure of 13KCl-CuCl; b) 13KCl-CuCl catalyzed dehydrochlorination for VDC; c) ΔG of $[\text{Cl-13KCl-CuCl}]^-$ catalyzed dehydrochlorination; d) ΔG of 13KCl-CuCl catalyzed acetylene hydrochlorination pathway.

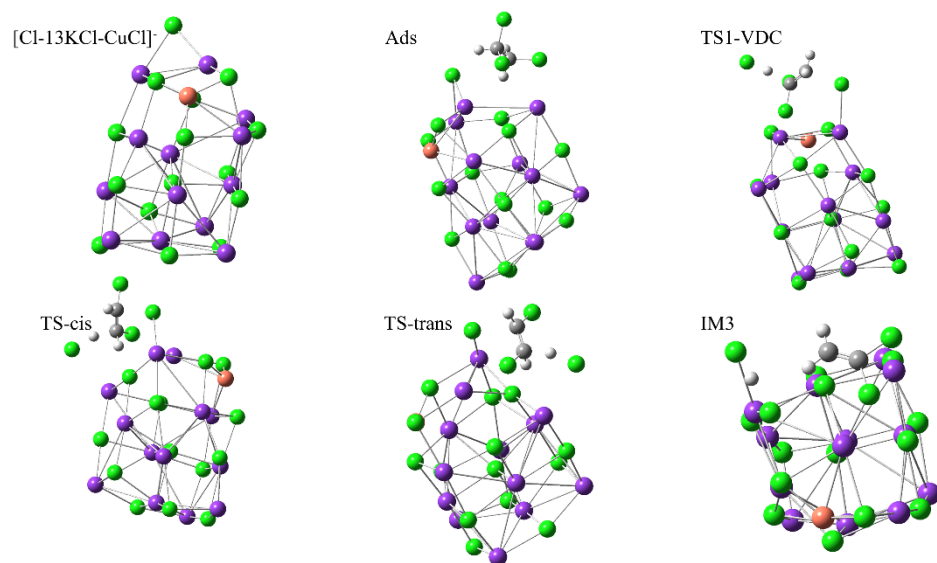


Figure S16. The structures of [Cl-13KCl-CuCl]⁻ catalyzed dehydrochlorination pathway.

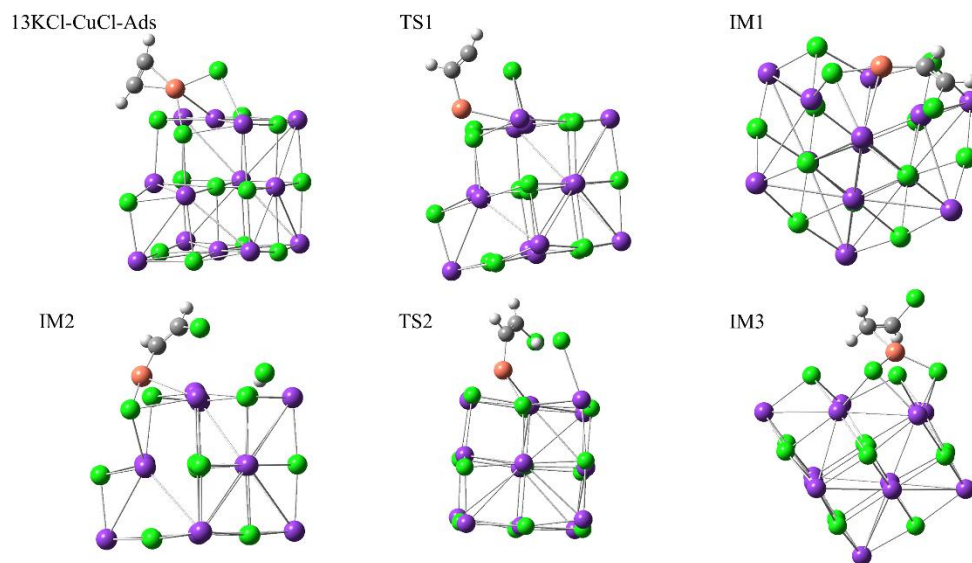


Figure S17. The structures of 13KCl-CuCl catalyzed acetylene hydrochlorination pathway.

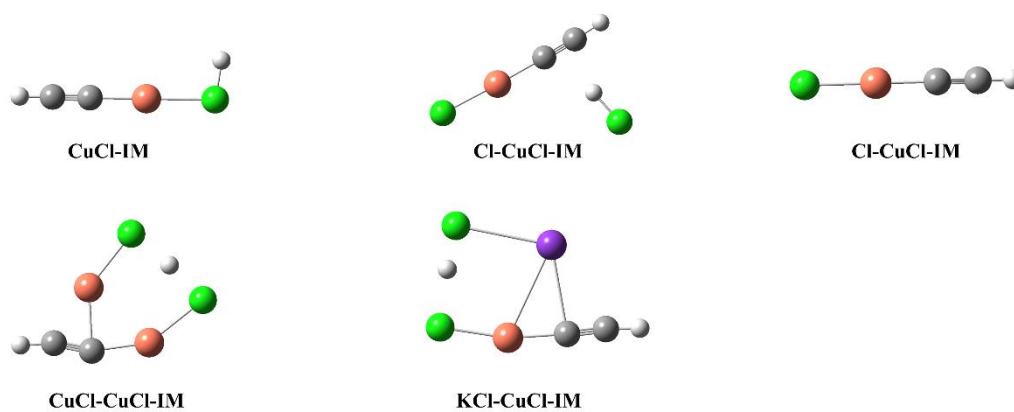


Figure S18. Partial structures in generation pathways of copper acetylide.

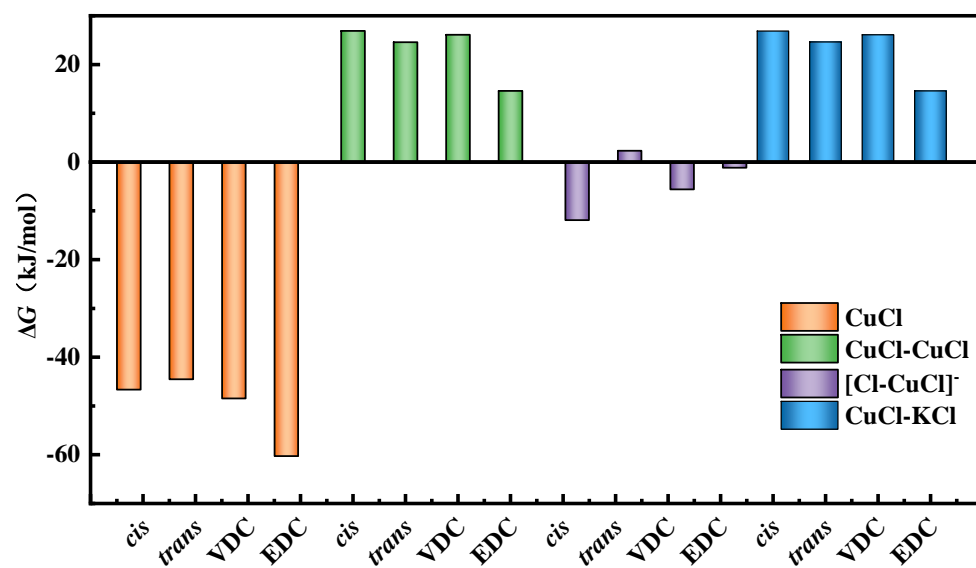


Figure S19. The adsorption ΔG of olefin products on CuCl, CuCl-CuCl and $[\text{Cl-CuCl}]^-$ at 260 °C.

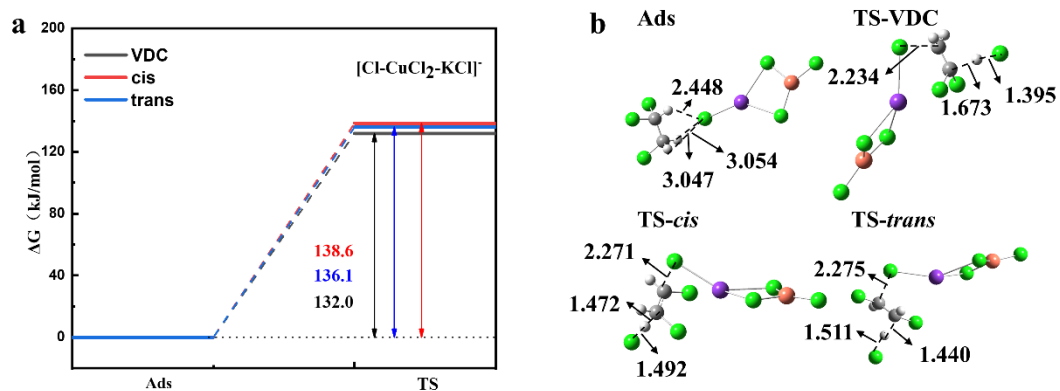


Figure S20. $[\text{Cl-CuCl}_2\text{-KCl}]^-$ catalyzed dehydrochlorination mechanism pathways at 260 °C: a) ΔG of $[\text{Cl-CuCl}_2\text{-KCl}]^-$ catalyzed mechanism; b) structures of adsorption and transition states $[\text{Cl-CuCl}_2\text{-KCl}]^-$ catalyzed mechanism.

Table S1. The adsorption $\Delta G_{20\text{ }^{\circ}\text{C}}$ and $\Delta G_{260\text{ }^{\circ}\text{C}}$ of HCl, C₂H₂ and TCE at TPPC-CuCl, TPPC-CuCl₂ and TPPC-KCl-CuCl. (kJ/mol)

	T/ $^{\circ}\text{C}$	HCl	C ₂ H ₂	TCE
TPPC-CuCl	20	-13.2	12.5	4.6
	260	13.0	-	-
[Cl-CuCl] ⁻	20	-39.7	-11.7	-34.2
	260	-27.7	-6.1	-20.9
TPPC-CuCl ₂	20	-9.2	12.2	-14.2
	260	18.6	-	20.1
TPPC-KCl-CuCl	20	-25.2	4.7	20.3
	260	4.5	-	-
[Cl-KCl-CuCl] ⁻	20	-52.6	-5.5	-25.5
	260	-24.4	23.0	-6.5
KCl-CuCl	20	-21.7	-38.6	6.6
	260	6.2	-9.3	-